

Investigation of the effect of autonomous vehicles (AV) on the capacity of an urban transport network

Ronald Nippold¹, Peter Wagner^{1,2}, Olaf Angelo Banse Bueno¹, and Christian Rakow²

¹ Institute of Transportation Systems, German Aerospace Center (DLR), Germany
ronald.nippold@dlr.de

² Department of Transport Systems Planning and Telematics, Technical University of Berlin, Germany

Abstract

In this paper, we assess the effects of different shares of autonomous vehicles (AVs) on the traffic flow and, in particular, on the maximum possible capacity at signal-controlled intersections. For this purpose, all signal-controlled nodes in the traffic network of the Düsseldorf metropolitan area were systematically simulated and evaluated using the microscopic traffic simulation tool SUMO.

The analysis shows that defensively parameterized AVs – as envisaged in the umbrella project of this research – may decrease the maximum possible traffic at signal-controlled intersections. Moreover, the simulation runs indicate that capacity at these intersections decreases almost linearly with a growing share of AV. In a second part of this analysis, a freeway section was simulated with the same varying shares of CV and AV to investigate free-flow traffic. In this case, the simulation results of the maximum traffic flow can be approximated by a third-order polynomial fit. The minimum capacity is found for the uniform share of both vehicle types (i. e. 50 % AV and 50 % CV).

The overall intent of this project is to provide an approach to determine system-wide and long-term effects of AVs from local microscopic observations. To this end, the SUMO microscopic traffic simulation will be utilized to derive realistic flow capacities for signal-controlled intersections. In a next step, these capacities will be transferred to a mesoscopic traffic simulation. Subsequently, flow capacities can be systematically adjusted in this network-wide mobility simulation to parameterize the influence of future infrastructure and vehicle technologies.

1 Introduction

Autonomous driving is gradually becoming an operational technology today. This development is anticipated to radically change the transportation sector in the coming years (ref. [1]). A number of expectations are associated with this process. As autonomous vehicles (AVs) are equipped with a variety of sensors and communication technologies, they are now assumed to further increase road safety compared to human-controlled conventional vehicles (CVs). At the same time, the overall traffic efficiency and thus traffic flow is projected to be improved due to the more homogeneous driving style of AVs compared to human drivers.

Currently, car manufactures are testing their Advanced Driver Assistance Systems (ADAS) as the first level of automation and – in some cases – even prototype vehicles of higher levels of automation¹. Partially, these pilot tests have already been carried out on publicly accessible

¹<https://www.sae.org/news/press-room/2018/12/sae-international-releases-updated-visual-chart-levels-of-driving-automation>

roads. For this purpose, test fields with intelligent infrastructure have been set up in a number of cities and regions².

However, there are still some open or not fully resolved issues that are subject of current research. A lot of work is spent on validation and verification of AVs [2, 3, 4]. In particular, this involves analyzing the artificial intelligence (AI) components, which are expected to replace human drivers as decision-makers in the future [5, 6]. In addition, aspects of cyber security in general or for specific components are also being intensively investigated [7, 8, 9]. On the side of (legal) regulations, there is also still a certain need for conclusive and complete regulations with regard to AVs [10, 11].

In particular, the ability of AVs to communicate with traffic infrastructure is expected to enable an “intelligent” and holistic decision-making process for traffic control. In the past, several algorithms for an optimized intersection control have been proposed in the literature [12, 13, 14, 15]. However, in the transition phase with mixed mode traffic, the capacity of roads and especially of intersections does not necessarily increase. Examples of mixed traffic can be found in the literature, in which AVs drive defensively with larger headways and thereby significantly reduce traffic flow and thus capacity at intersections [16] and on freeways [17].

There is still no clear picture of how traffic capacities will develop in the future, especially during the transition phase with an increasing share of AVs. For this reason, the paper investigates the flow capacities at signal-controlled intersections of a real-world road network of a metropolitan area with different shares of AV and CV in a systematical manner. This analysis is part of an approach to determine system-wide and long-term effects of AVs from local microscopic observations. For this purpose, the microscopic simulation “SUMO” [18] is integrated in a framework with the mesoscopic agent-based mobility-simulation “MATSim” [19] to derive realistic flow capacities for traffic signal-controlled intersections for different shares of CV and AV. This framework is applied to systematically adjust and parameterize the effect of future infrastructure and vehicle technologies in the network of the greater Düsseldorf area in Germany, which is part of the German national test field for automated and connected driving³.

2 Scenario overview

The following section illustrates the analyzed road network and lists all required components to build and simulate the virtual representation of the scenario.

2.1 Simulation network

As the basis for this research, a raw OSM (openstreetmap⁴) road network of the greater Düsseldorf area was imported into SUMO. Due to the dimensions of this network (area: approximately 900 km², total length of all edges: about 13700 km, number of signal-controlled intersections: 1637), post-processing and quality control were generally omitted. Figure 1 on the facing page shows the network and its expanse. The city of Düsseldorf can be recognized by the close meshed road network in the center of the picture.

²For an overview of the situation in Germany cf. e.g. <https://www.bmvi.de/DE/Themen/Digitales/AVF-Forschungsprogramm/Projekte/avf-projekte> (German language only).

³<https://komodnext.org/>

⁴<https://www.openstreetmap.org>

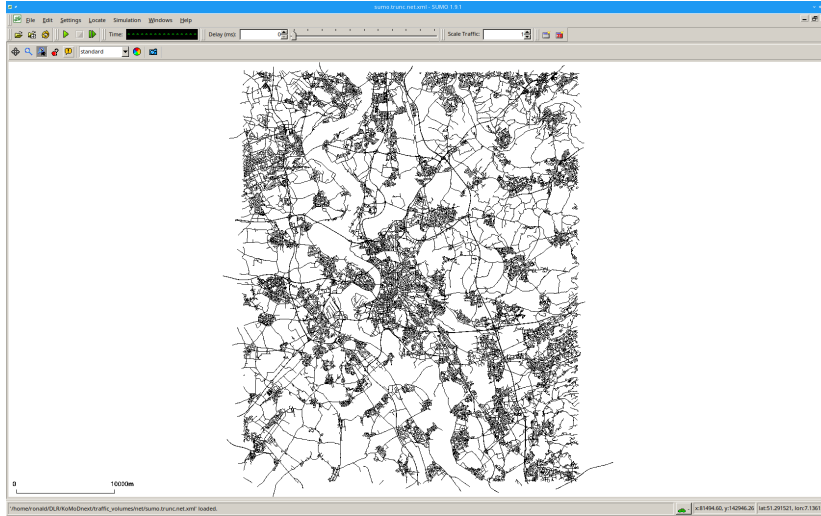


Figure 1: Dimension of the simulation network under investigation. The city of Düsseldorf is situated in the center of the network. The broad, curving and road-free band running vertically through the network is the river Rhine.

2.2 Driver models parameters

For the present analysis, the SUMO implementation of the KRAUSS model was used for simulating the vehicle behavior due to its simplicity and reliability. This model, as documented in [20], is used as the default car-following model in SUMO. It is a space-continuous model based on a safe speed definition. As an advantage, the model needs only a moderate set of input parameters in comparison to other car-following models, e. g. the WIEDEMANN model used in VISSIM [21] or the standard model of the MITSIM simulator [22].

For the analysis, CVs were simulated using SUMO’s default parameter set for passenger cars (cf. the second column of Tab. 1). As shown in the third column of this table, the parameters for the AV were adapted appropriately. For technical reasons, the deceleration of AV in normal

Table 1: Parameter set for modeling CV and AV. CV corresponds to the SUMO default parameter set and is only displayed for easy comparison. All other model parameters not listed in this table correspond to their respective SUMO default values.

Parameter	CV (default)	AV (adapted)
decel	7.5	3.0
tau	1	1.5
sigma	0.5	0.1
speedFactor	1	1
speedDev	0.1	0

mode is limited to $b = 3.0 \text{ m/s}^2$. Note that there is another emergency breaking mode for AVs, which allows a much higher braking deceleration. The driver’s desired (minimum) time headway τ refers to the net space between leader back and follower front. AVs were simulated rather conservative with a time headway of $\tau = 1.5 \text{ s}$ reflecting the specifications used in the umbrella project. Note that τ may possibly decrease by several orders of magnitude as technology of AVs advances and the regulatory environment changes. However, the regulatory framework is still not fully defined. The driver imperfection σ reflects small deviations and defects that human driver usually introduces into car-following mode due to variations in perception or concentration. A value of $\sigma = 0$ denotes perfect driving without any deviations. The value of $\sigma = 0.1$ is again chosen rather conservative and reflects the occurrence of latencies in the internal signal processing modules of AVs. The parameters `speedFactor` and `speedDev` indicate the mean and variance of a possible speed deviation, i. e. whether drivers generally exceed or fall below the defined lane speed. According to Tab. 1, AVs drive always with the intended or permissible speed.

Any other vehicle classes – e. g. motorbikes, buses and trucks – were neglected in the investigations. Lane changing is also not integrated into the analysis, as the aim was to study vehicle flow in a single driving or turning lane in front of signal-controlled intersections. In addition, no V2X communication or other AV concepts such as platooning etc. were applied, as their use is also not planned in the umbrella project.

2.3 Simulation setup

The road network contains 1637 signal-controlled nodes, which in turn are divided into 17653 driving or turning lanes. The traffic signals in this network were modeled as traffic actuated units. In this way, the traffic signals react to the magnitude of the respective traffic flows. Each lane at these traffic signal-controlled intersections was simulated separately in SUMO with different shares of CV and AV to determine the maximum possible traffic flow. For this purpose, the SUMO interface TraCI (traffic control interface) was used, which allows interacting with a running traffic simulation and modifying objects and their behavior.

In a first step, the network was loaded and parsed with the Python module `sumolib`. All signal-controlled intersections were identified and their IDs were stored in a list. Internal intersections (i. e. the waiting positions within the intersection) were ignored. The actual determination of capacities was then performed iteratively using a Python script and TraCI for each of the previously stored intersection IDs. This involved looping through each possible lane of each identified intersection ID and creating a route file with a vehicle flows for a variable share of CV and AV. The overall traffic volume was set to 2000 veh/h for that specific lane (sum of CV and AV share). Respective “e1”-detectors with a frequency of 1 sec were defined in SUMO for this connection. Finally, the simulation was run for one hour using the route and detector files generated above as inputs. To ensure a faster procedure, the list of intersections to be processed was divided and manually distributed to the available CPU cores of a server. The size of the road network and thus the required working memory played an important role and limited the number of possible parallel runs.

The detector outputs, resulting from all the simulations performed, had all their file names corresponding to the connections they were scrutinizing. Subsequently, an R-script was developed to extract the data from all of these detector output files, determine the traffic volumes relative to an hour, and summarize the results.

3 Relationship between road capacity and headways

The following section gives a brief description of the relationship between road capacity q , speed v and headways T in the vehicle flow. The capacity c generally corresponds to the maximum traffic flow q_{\max} that a traffic flow can reach at a given road section under defined environmental and traffic conditions. The traffic flow q is defined as the number of vehicles per unit of time. The smallest possible unit of q is the inverse gross headway T_g of a vehicle:

$$q = \frac{1}{T_g} = \frac{v}{v \cdot T + l}. \quad (1)$$

The gross headway T_g itself is defined as the space $d = v \cdot T + l$ that is occupied by a car; where T is the net time headway and l is the generalized car-length, i. e. physical length of the car plus the additional free space occupied in a jam.

The traffic flow q as a function of the speed v is a monotonously increasing function, as shown in Fig. 2. Eq. (1) can be rewritten into the more familiar $v(q)$ -form:

$$v(q) = \frac{q \cdot l}{1 - q \cdot T}. \quad (2)$$

This corresponds to the congested arm of the FD (rf. [23]). The free arm is a declining function of speed v versus demand q , at least for heterogeneous car-fleets with different preferred speeds of the vehicles:

$$v(q) = v_{\text{free}} \left(1 - \frac{q}{q_0} \right). \quad (3)$$

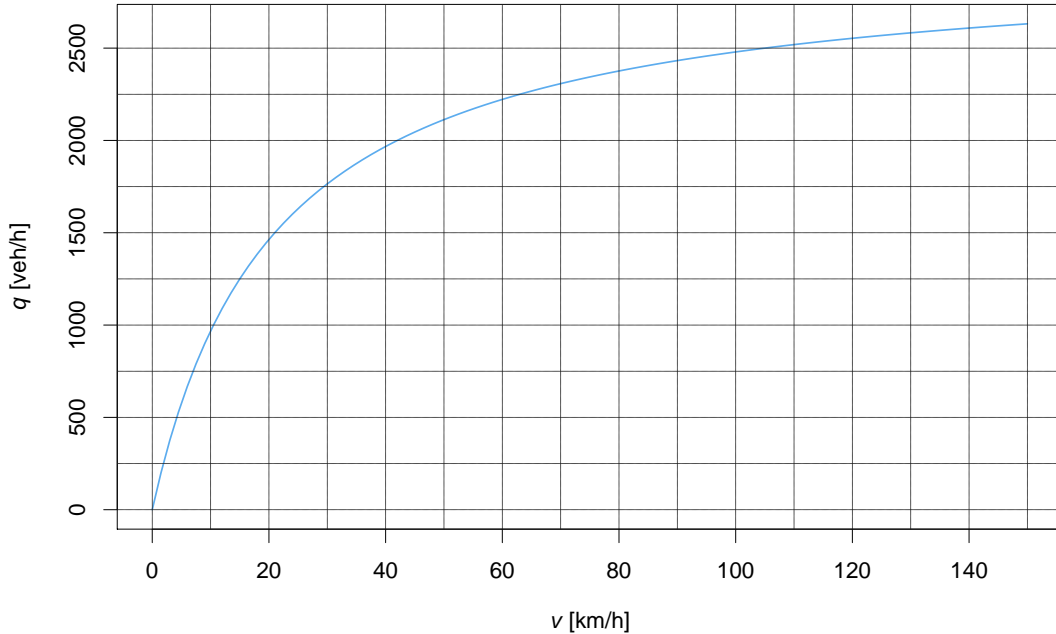


Figure 2: Monotonous increasing capacity q vs. speed v curve.

Note, eq. (3) can be simplified for homogeneous fleets as follows:

$$v(q) = v_{\text{free}}. \quad (4)$$

Therefore, the full definition of the FD as a combination of eqn. (3) and (4) reads:

$$v(q) = \begin{cases} v_{\text{free}} \left(1 - \frac{q}{q_0}\right) & \text{if } v > v_c \\ \frac{q \cdot l}{1 - q \cdot T} & \text{if } v \leq v_c \end{cases}. \quad (5)$$

The capacity versus speed curve in Fig. 2 is valid under the assumption that all vehicles in a given traffic stream follow each other with the optimal distance $v \cdot T$. Of course, this would require that the distance T is independent of the velocity v . However, the validity of this assumption is not guaranteed.

Eq. (1) can be easily generalized or adapted to a fleet of different vehicles; where each vehicle type i is characterized by its length l_i , the headway T_i and a respective share p_i ($\sum_i p_i = 1$). This results in a more complex formulation of Eq. (1) as follows:

$$q_c = \frac{v}{\sum_i p_i (v \cdot T_i + l_i)}. \quad (6)$$

The assumption that AVs follow each other (if this information is distributed via V2V communication) at a shorter distance, but increase their headway in case of CV as leading vehicle, can be modeled with a similar approach. At least three different distances are introduced then: T_{aa} , T_{ah} , T_{hx} ; where the first index denotes the following and the second index the leading vehicle. If θ denotes the share of AV, Eq. (6) can be rearranged as follows (assuming one generalized vehicle length l):

$$q_c = \frac{v}{l + v \left(\theta^2 \cdot T_{aa} + (1 - \theta)^2 T_{hh} + \theta (1 - \theta) (T_{ah} + T_{ha}) \right)}. \quad (7)$$

4 Results

This section presents the maximum possible capacities observed at the signal-controlled intersections in the simulations for the greater Düsseldorf area. For this analysis, the share of AV was increased by 10% steps reaching from 0% up to 100%. CV and AV were parameterized and modeled according to Tab. 1 in subsection 2.2.

4.1 Signal-controlled intersections

Fig. 3 on the next page gives an overview of the determined maximum capacities q on all lanes of all signal-controlled intersections in vehicles per hour for the 11 different shares of CV and AV. In general, the distributions obtained correspond to the expected assumptions, especially for the case of pure CV traffic (cf. the dashed blue curve in Fig. 3). The mean value for 100% CV equals $\bar{q} = 1131 \text{ veh/h}$, the minimum value is $q_{\text{min}} = 24 \text{ veh/h}$ and the maximum value reaches $q_{\text{max}} = 1766 \text{ veh/h}$. There is a total amount of 20 cases (i. e. lanes of signal-controlled intersections) with unrealistic low values of $q < 100 \text{ veh/h}$. These values are caused by network errors in the unprocessed OSM network. Fig. 4a on the facing page contains an example for an intersection with partial lane defects that significantly impact traffic flow. For the case of 100% CV, the traffic flow exceeds a value of $q > 1600 \text{ veh/h}$ for 369 lanes. Such high values at

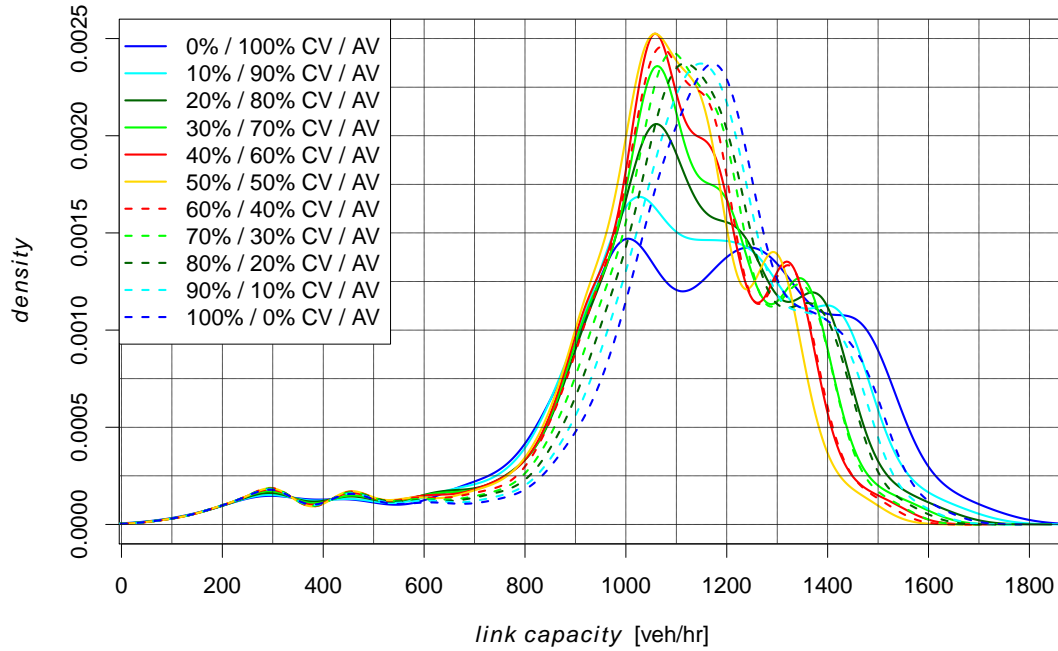


Figure 3: Density curves of the theoretical maximum traffic flows for all lanes in front of all 1637 traffic signal-controlled intersections in the study area. The different penetration rates of AVs are reflected by different colors and line types. Note that higher percentages of AVs are shown as solid lines, while lower AV rates (and thus higher rates of CV) are drawn as dashed curves.

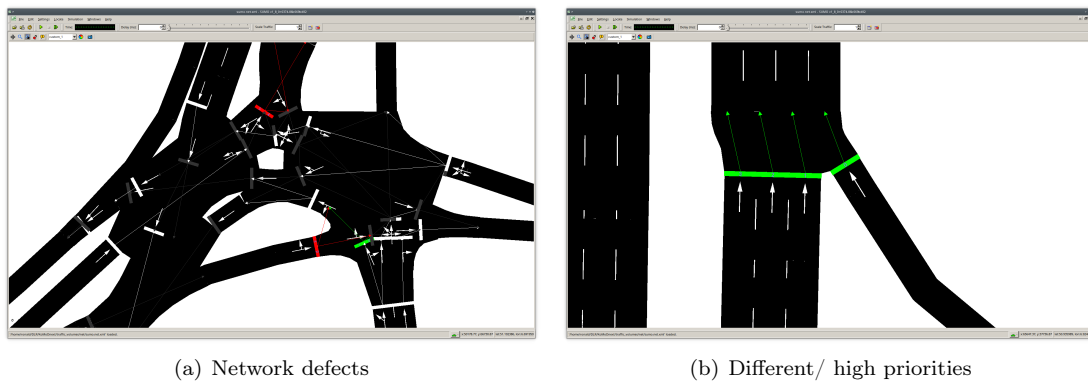


Figure 4: Example of an intersection with network defects and thus significantly reduced traffic flows (a). Example of traffic lights at a junction of roads with different priorities or road categories (b). Link indices 1 to 3 on the northbound main road have a higher priority and therefore a potentially higher traffic flow.

urban intersections are not quite unrealistic. Generally, these values represent special cases of intersections with different road categories. Fig. 4 b shows an example where vehicles traveling northbound on the three-lane main road can simply continue straight ahead at normal speed when the traffic light is green. These vehicle do not have to reduce their speed, as is the case at other intersections, e. g. when turning left or right.

Fig. 5 shows the range of the peak values ($1000 \text{ veh/h} < q < 1200 \text{ veh/h}$) of the density curves of Fig. 3 in greater details. With an increasing share of CV traffic (dashed lines in Fig. 5), the peaks shift to the right side into the area of higher capacity resp. traffic flow. This effect can be observed even better in Fig. 6 on the facing page.

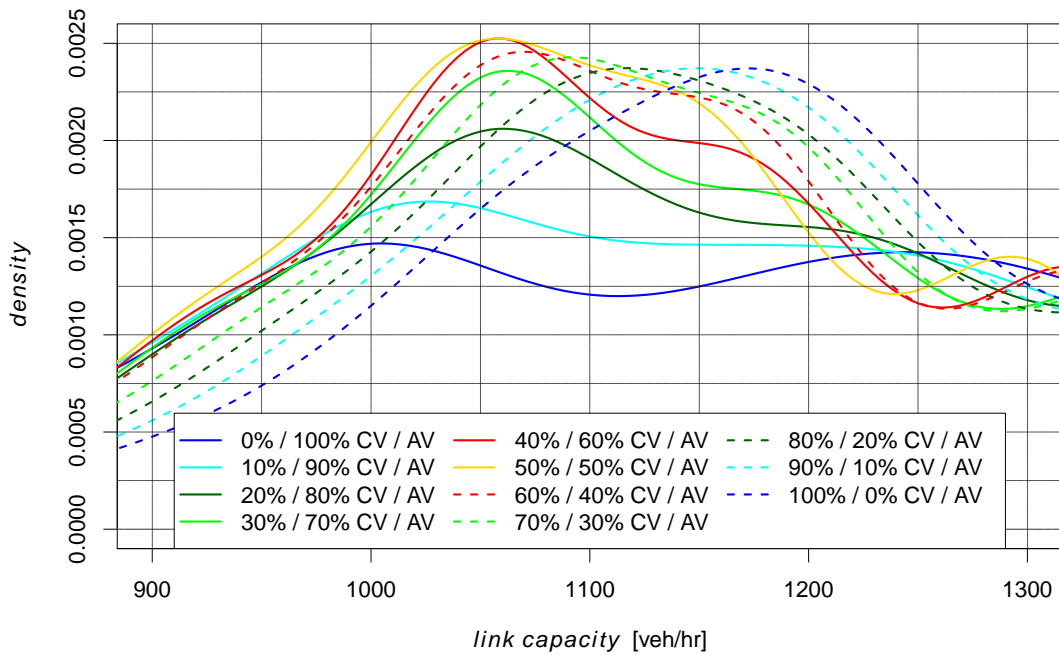


Figure 5: Detail of the peak values of the density curves of the theoretical maximum traffic flows for all lanes in front of all 1637 traffic signal-controlled intersections in the study area.

This diagram presents a linear fit of the class means of the maximum traffic flow rate q for the 11 analyzed distributions of CV and AV. The x -axis represents the share of CVs in the simulated traffic flows. The share of AVs is correspondingly reciprocal. Obviously, the class means of the maximum traffic flow rate q increase almost linearly with a growing share of CVs. Only the class mean for the uniform distribution of both types of vehicle (i. e. 50 % AV and 50 % CV) deviates slightly from this linear relationship. This behavior may be caused by the maximum degree of disruption in traffic flow introduced by the two different driving regimes of AV and CV. The class means of the maximum traffic flow rate of 100 % AV ($q = 1010 \text{ veh/h}$) and 100 % CV ($q = 1170 \text{ veh/h}$) differ noticeably by over 10 %.

As a consequence, this means that road capacities decrease as the number of AVs increases. This finding is in line with an analysis of Mattas et al. [24] who conducted a simulation study for AVs and connected autonomous vehicles (CAV) using a model proposed by Shladover et al. [25]. This study evaluates effects of connectivity and automation on the Antwerp ring road in Belgium. The results demonstrate that AVs can have a negative impact on the traffic flow q ,

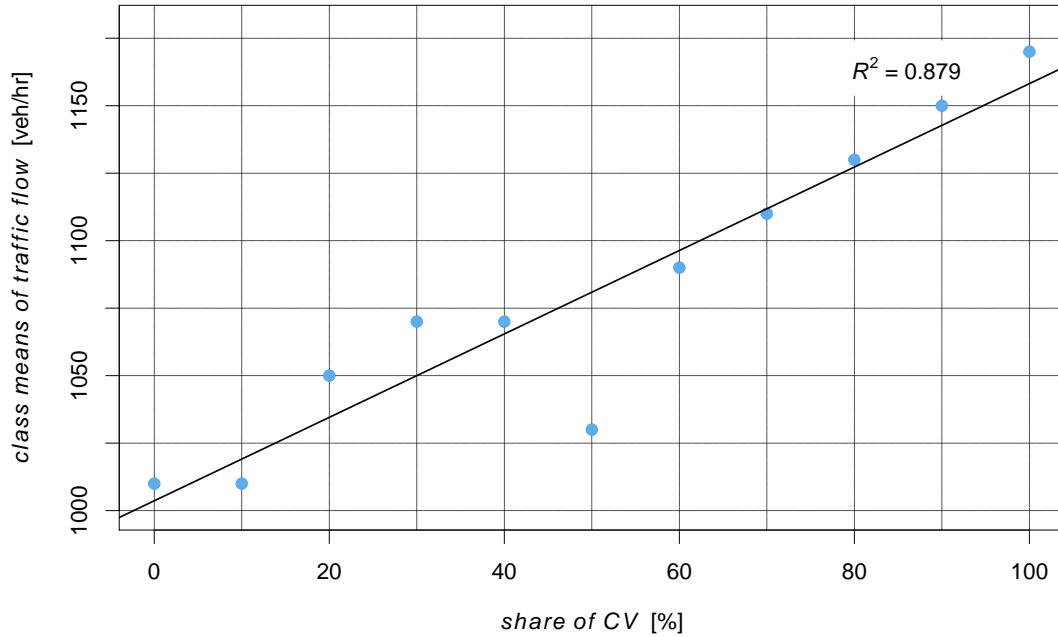


Figure 6: Linear fit of the class means of the peak capacities for the analyzed distribution of CV and AV at signal-controlled intersections. The x -axis denotes the share of CV, the share of AV is correspondingly reciprocal to it.

depending on the overall traffic demand. The connectivity and the exchange of traffic messages through CAVs have emerged as key elements for achieving higher network capacities. As a result of the reduction in capacity due to AVs, travel times for motorized individual transport also increase. Accordingly, individual transport would become less attractive overall due to the potentially greater volume of congestion. This should ultimately affect the modal split in the study area.

However, it must be pointed out that the study was concerned with the maximum possible flow. In reality, traffic is not at the limit at all times and in all places. Also, the quite conservatively dimensioned vehicle parameters of the AVs only represent a current interim status and not the final technological development. In this direction, further improvements are to be expected in the future. In addition, it must also be taken into account that there is currently no conclusive legal framework that bindingly outlines a safe parameter range for AVs.

4.2 Freeway

The situation described in the previous section is characterized by very high traffic demand at signal-controlled intersections. The traffic flow is interrupted at more or less regular intervals by the necessary activation of the transverse direction. Free traffic flow and thus car-following only occurs in certain intervals of time.

For this reason, the capacity impact of the 11 evaluated distributions of CV and AV was investigated for a car-following situation on a freeway section in the test area. The selected road section was the approx. 5.5 km long segment of the BAB 57 between the interchanges

“Meerbusch” and “Kaarst” in the west of Düsseldorf. The autobahn has three lanes, and the maximum speed is 100 km/h. The terrain is very flat, the road gradient is less than 1 %.

According to the HBS (German “Handbuch für die Bemessung von Straßenverkehrsanlagen”) [26], the maximum traffic flow on a comparable road section within metropolitan areas and without heavy duty traffic is $q_{\max} = 5700$ veh/h. The Swiss “Bundesamt für Strassen” calculates with $q_{\max} = 5800$ veh/h for equivalent road sections and circumstances [27]. Therefore, this road section was simulated with the same shares of AV and CV, the same model parameter sets according to Tab. 1 and a traffic demand of $q = 5800$ veh/h. In accordance with Fig. 6, the class means of the determined maximum traffic flow rate q are presented in Fig. 7 for the freeway scenario. Again, the x -axis denotes the share of CVs in the simulated traffic flows. The share of AVs is correspondingly reciprocal.

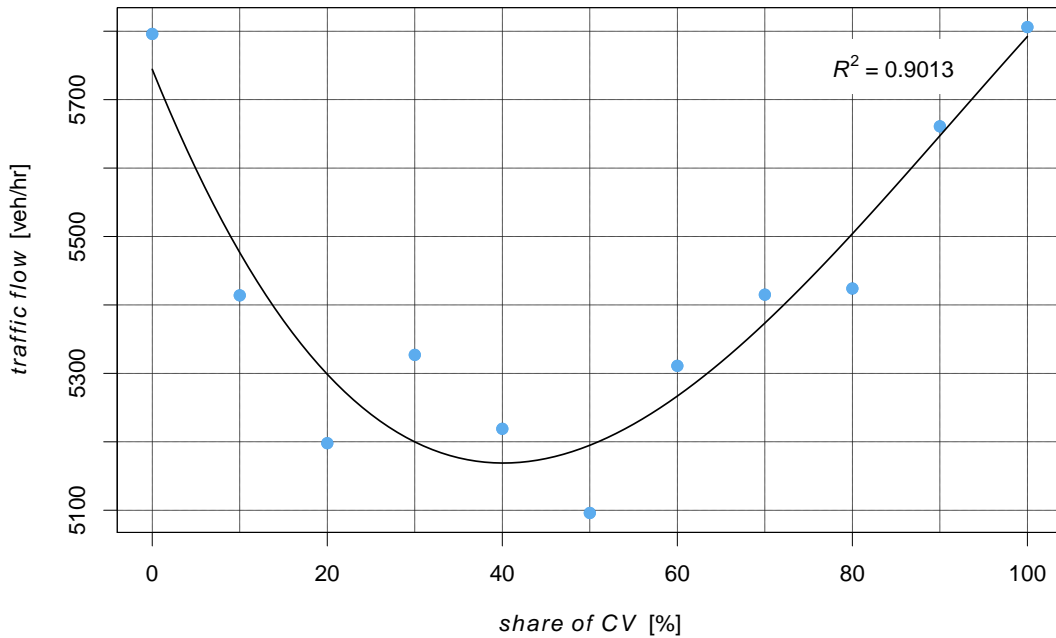


Figure 7: Third order polynomial fit of the class means of the peak capacities for the analyzed distribution of CV and AV for freeway traffic. The x -axis denotes the share of CV, the share of AV is correspondingly reciprocal to it.

In contrast to the case of the signal-controlled intersections, the resulting point cloud of class means of the maximum traffic flow q can be approximated by a third-order polynomial fit in a reasonable way. The uniform distribution of both vehicle types (i. e. 50 % AV and 50 % CV) leads to a minimum traffic flow of $q = 5096$ veh/h.

The maximum traffic flow rates can be observed for both AV-only and CV-only traffic. The maximum class mean for 100 % AV is only very slightly higher ($q = 5806$ veh/h) compared to 100 % CV ($q = 5796$ veh/h). Note that the class means of the maximum traffic flow q themselves and consequently the fitting curve are not symmetric. This implies a larger increase in road capacity resp. traffic flow rate q with a growing share of AV than for the case of an increased CV rate. Thus, a quadratic fit of the resulting point cloud only achieves a worse coefficient of determination ($R^2 = 0.8642$) than a third order polynomial fit ($R^2 = 0.9013$). The reason for

this can be assumed to be the smoother traffic flow with a higher share of automated vehicles exhibiting a well defined and uniform driving behavior. The simulation of the free-flow traffic on the freeway segment shows that the larger headways of the AVs lead to decreased road capacities only in conjunction with the disrupted traffic flow at signal-controlled intersections.

5 Conclusion

The aim of this study is to assess the effects of different shares of AVs on the traffic flow and, in particular, on the maximum possible capacity at signal-controlled intersections. Therefore, all signal-controlled nodes in the traffic network of the Düsseldorf metropolitan area were systematically simulated and evaluated using the microscopic traffic simulation tool SUMO.

This analysis is the basis for an approach to determine system-wide and long-term effects of AVs from local microscopic observations. The microscopic transport simulation SUMO is utilized to derive realistic flow capacities for signal-controlled intersections. These capacities are transferred to the mesoscopic transport simulation MATSim and then systematically adjusted to parameterize the effect of future infrastructure and vehicle technologies.

The analysis shows that defensively parameterized AVs – as foreseen in the umbrella project of this research – may decrease the maximum possible traffic at signal-controlled intersections. Moreover, the simulation runs reveal that capacity at these intersections decreases almost linearly with a growing share of AV. The observed class means of the maximum traffic flow rate of 100 % CV ($q = 1170 \text{ veh/h}$) and 100 % AV ($q = 1010 \text{ veh/h}$) differ noticeably by over 10 %. Similar results can be found in the literature, e. g. in [16].

Because the traffic flow at signal-controlled intersections is interrupted at more or less regular intervals, car-following can only occur at specific, relatively short time intervals. For this reason, a freeway section was analyzed with the same varying shares of CV and AV in the second part of this analysis. The traffic flow corresponded to the theoretical maximum traffic volume of $q_{\max} = 5800 \text{ veh/h}$ for a comparable road section without heavy goods traffic. In contrast to signal-controlled intersections, a minimum traffic flow rate $q = 5096 \text{ veh/h}$ is found for a uniform share of both vehicle types (i. e. 50 % AV and 50 % CV). The maximum traffic flow rate ($q \approx 5800 \text{ veh/h}$) emerges for both AV-only and CV-only traffic; the deviations between these configurations are negligible. The simulation results of the maximum traffic flow q can be approximated by a third-order polynomial fit.

As a next step, it is planned to model intelligent traffic infrastructure concepts directly in SUMO and transfer adapted capacities to the mesoscopic simulation MATSim. This allows for an improved investigation of such technologies and provides the basis for an economic evaluation of an infrastructure roll-out. With access to the national test-field in Düsseldorf, we also plan to test some of these intelligent infrastructure concepts in practice and validate the obtained simulation results.

ACKNOWLEDGMENT

Our special thanks go to the “KoMoDnext” project founded by the German Federal Ministry of Transport and Digital Infrastructure for kindly providing the demand data set.

References

- [1] Maria Alonso Raposo, Biagio Ciuffo, Fulvio Ardenete, Jean Philippe Aurambout, Gianmarco Baldini, Robert Braun, Panayotis Christidis, Aris Christodoulou, Amandine Duboz, Sofia Felici, et al. The future of road transport. Technical report, Joint Research Centre (Seville site), 2019.
- [2] Nijat Rajabli, Francesco Flammini, Roberto Nardone, and Valeria Vittorini. Software verification and validation of safe autonomous cars: A systematic literature review. *IEEE Access*, 9:4797–4819, 2021.
- [3] Dhanoop Karunakaran, Stewart Worrall, and Eduardo M. Nebot. Efficient statistical validation with edge cases to evaluate highly automated vehicles. *CoRR*, abs/2003.01886, 2020.
- [4] Juozas Vaicenavicius, Tilo Wiklund, Austé Grigaitė, Antanas Kalkauskas, Ignas Vysniauskas, and Steven Keen. Self-driving car safety quantification via component-level analysis. *SAE Intl. J CAV*, 4:35–45, April 2021.
- [5] G Baldini. Testing and certification of automated vehicles (av) including cybersecurity and artificial intelligence aspects. 2020.
- [6] Chih-Hong Cheng and Rongjie Yan. Continuous safety verification of neural networks, October 2020.
- [7] Gurcan Comert, Mashrur Chowdhury, and David M. Nicol. Assessment of system-level cyber attack vulnerability for connected and autonomous vehicles using bayesian networks. *CoRR*, abs/2011.09436, 2020.
- [8] Shahida Malik and Weiqing Sun. Analysis and simulation of cyber attacks against connected and autonomous vehicles. In *2020 International Conference on Connected and Autonomous Driving (MetroCAD)*, pages 62–70. IEEE, February 2020.
- [9] Rony Komissarov and Avishai Wool. Spoofing attacks against vehicular fmcw radar, April 2021.
- [10] Steven Uytsel. Testing autonomous vehicles on public roads: Facilitated by a series of alternative, often soft, legal instruments. In Steven Van Uytsel and Danilo Vasconcellos Vargas, editors, *Autonomous Vehicles, Perspectives in Law, Business and Innovation*, pages 39–64. Springer, May 2021.
- [11] Markus Maurer, J. Gerdes, Barbara Lenz, and Hermann Winner. *Autonomous Driving. Technical, Legal and Social Aspects*. 05 2016.
- [12] Darshan Gadginmath and Pavankumar Tallapragada. Data-driven distributed intersection management for connected and automated vehicles, July 2020.
- [13] Tanja Niels, Klaus Bogenberger, Nikola Mitrovic, and Aleksandar Stevanovic. Integrated intersection management for connected, automated vehicles, and bicyclists. In *2020 IEEE 23rd International Conference on Intelligent Transportation Systems (ITSC)*, pages 1–8. IEEE, September 2020.
- [14] Youssef Bichiou and Hesham A. Rakha. Developing an optimal intersection control system for automated connected vehicles. *IEEE Trans. Intell. Transp. Syst.*, 20(5):1908–1916, 2019.
- [15] Joyoung Lee and Byungkyu Park. Development and evaluation of a cooperative vehicle intersection control algorithm under the connected vehicles environment. *IEEE Trans. Intell. Transp. Syst.*, 13(1):81–90, 2012.
- [16] Scott Le Vine, Alireza Zolfaghari, and John Polak. Autonomous cars: The tension between occupant experience and intersection capacity. *Transportation Research Part C: Emerging Technologies*, 52:1–14, 03 2015.

- [17] Mohamed Berrazouane, Kailin Tong, Selim Solmaz, Martijn Kiers, and Jacqueline Erhart. Analysis and initial observations on varying penetration rates of automated vehicles in mixed traffic flow utilizing sumo. In *ICCVE*, pages 1–7. IEEE, 2019.
- [18] Pablo Alvarez Lopez, Michael Behrisch, Laura Bieker-Walz, Jakob Erdmann, Yun-Pang Flötteröd, Robert Hilbrich, Leonhard Lücken, Johannes Rummel, Peter Wagner, and Evamarie Wiessner. Microscopic traffic simulation using sumo. In *2018 21st International Conference on Intelligent Transportation Systems (ITSC)*, pages 2575–2582. IEEE, November 2018.
- [19] Kay W Axhausen, Andreas Horni, and Kai Nagel. The multi-agent transport simulation matsim, 2016.
- [20] S. Krauß. *Microscopic modelling of traffic flow: Investigation of Collision Free Vehicle Dynamics*. PhD thesis, University of Cologne, 1998.
- [21] Rainer Wiedemann. Simulation des Straßenverkehrsflusses. Technical report, Institut für Verkehrswesen, Universität Karlsruhe, 1974. Heft 8 der Schriftenreihe des IfV, in German.
- [22] K. I. Ahmed. *Modelling Drivers' Acceleration and Lane-Changing Behavior*. PhD thesis, MIT, 1999.
- [23] 75 years of the fundamental diagram for traffic flow theory - greenshields symposium, 2011.
- [24] K. Mattas, M. Makridis, P. Hallac, M. A. Raposo, C. Thiel, T. Toledo, and B. Ciuffo. Simulating deployment of connectivity and automation on the antwerp ring road. *IET INTELLIGENT TRANSPORT SYSTEMS*, 12(9):1036–1044, 2018.
- [25] Steven E. Shladover, Dongyan Su, and Xiao-Yun Lu. Impacts of cooperative adaptive cruise control on freeway traffic flow. *Transportation Research Record*, 2324(1):63–70, 2012.
- [26] *HBS – Handbuch für die Bemessung von Straßenverkehrsanlagen*. Number ISBN: 978-3-86446-103-3. FGSV Verlag – Der Verlag der Forschungsgesellschaft für Straßen- und Verkehrswesen, 2015.
- [27] H. Werdin, H. Honermann, R. Laube, and I. Belopitov. *Verkehrsqualität und Leistungsfähigkeit auf Autobahnen*. 2004.